Dynamics of plankton growth in the Barents Sea: model studies

DAG SLAGSTAD and KJELL STØLE-HANSEN

1-D and 3-D models of plankton production in the Barents Sea are described and a few simulations presented. The 1-D model has two compartments for phytoplankton (diatoms and *P. pouchetii*), three for limiting nutrients (nitrate, ammonia and silicic acid), and one compartment called "sinking phytoplankton". This model is coupled to a submodel of the important herbivores in the area and calculates the vertical distribution in a water column. Simulations with the 3-D model indicate a total annual primary production of 90–120 g C m^{-2} yr^{-1} in Atlantic Water and 20–50 g C m^{-2} yr^{-1} in Arctic Water, depending on the persistence of the ice cover during the summer.

The 3-D model takes current velocities, vertical mixing, ice cover, and temperature from a 3-D hydrodynamical model. Input data are atmospheric wind, solar radiation, and sensible as well as latent heat flux for the year 1983. The model produces a dynamic picture of the spatial distribution of phytoplankton throughout the spring and summer. Integrated primary production from March to July indicates that the most productive area is Spitsbergenbanken and the western entrance to the Barents Sea, i.e. on the northern slope of Tromsøflaket.

Dag Slagstad and Kjell Støle-Hansen, SINTEF Automatic Control, N-7034 Trondheim-NTH, Norway.

Introduction

The growth of phytoplankton depends strongly on physical factors such as light and the vertical stability of the water column. These processes have a strong seasonal and spatial variability in the Barents Sea. A necessary condition for the start of a phytoplankton bloom is that the depth of surface mixing is less than the critical depth (i.e. where depth-integrated losses equal growth, Sverdrup 1953). On the other hand, if the water column is too stable, the supply of nutrients from deeper water masses is inhibited and the post-bloom production becomes very low.

The Barents Sea is well north of the Arctic Circle where the sun is always below the horizon during mid-winter but constantly above the horizon during the summer. Clouds and fog reduce incident light to about half of that on cloudless days (Sakshaug & Slagstad 1991 this volume).

The Norwegian Coastal Current enters the Barents Sea near the coast of Norway and may stabilise due to the fresh water runoff. In the northern part, melting of ice releases freshwater and creates a stable water column. Between these two water masses, Atlantic Water enters the Barents Sea from the west. This water has a high salinity and is little affected by fresh water input. The main stabilisation factor here is the heating of the surface layer.

The main herbivores are *Calanus finmarchicus* in the Atlantic part and *C. glacialis* in the Arctic part of the Barents Sea. *C. finmarchicus* has a one-year life cycle whereas *C. glacialis* requires two years to complete one life cycle (Tande et al. 1985). Because the zooplankton models have been described elsewhere (Slagstad & Tande 1990; Tande & Slagstad 1991), we will concentrate on the dynamics of phytoplankton and nutrients here.

The phytoplankton community is dominated by one or several species of diatoms (*Chaetoceros socialis, C. furcellatus, Nitzschia grunowii* and *Thalassiosira nordenskioeldii*) and solitary cells or colonies of the prymnesiophyte *Phaeocystis pouchetii*. These algae may accumulate in the upper water mass in concentration reaching > 10 mg Chl *a* m^{-3} during the peak of the blooms (Båmsted et al. 1991, this volume).

The mathematical modelling of the Barents Sea ecosystem started in 1976 (Balchen 1980; Slagstad 1981). These early efforts were based on data from published studies which were not always easy to apply to a subarctic ecosystem. During the Pro Mare programme, far more biological

data became available, some of which have been incorporated into the model. There are, however, still important parts of the ecosystem (for example krill, the microbial loop, and ciliates) which have not yet been implemented into the model.

The purpose of this paper is to describe the plankton model and to show simulations that illustrate the overall features of the plankton production in different regions of the Barents Sea. A 1-D model is used for simulation of typical situations in the Atlantic and Arctic regions of the Barents Sea, whereas a 3-D model with partly realistic input (wind, atmospheric pressure, and solar radiation) is used to simulate the spatial distribution of phytoplankton during the spring and summer.

The 1-D model is comprehensive and includes many features which are beyond the main purpose of this paper and, thus, not demonstrated by simulations here. The dynamics of diatoms and *P. pouchetii* populations are shown in Båmstedt et al. (1991 this volume).

Model formulation

1-D model

A 1-D model is based on the assumption that horizontal gradients of biological and physical variables are small enough to be neglected. The important hydrodynamical processes are vertical turbulent mixing and vertical advection:

$$\frac{\partial \theta}{\partial t} + w \frac{\partial \theta}{\partial z} - \frac{\partial}{\partial z} \left(K_z \frac{\partial \theta}{\partial z} \right) = f_{biol}^\theta \qquad (1)$$

where $\theta(t,z)$ is the concentration of a constituent (phytoplankton, nutrients or temperature) at the depth z and time t; w is the vertical velocity (usually sinking velocity); $K_z(z,t)$ is the vertical turbulent mixing coefficient; and f_{biol}^θ is a function that determines the rate of local production of a constituent, usually as a consequence of biological or chemical activity, here called the "biological term".

This model contains one coefficient that is determined by hydrodynamics alone (K_z) and one as a result of combined biological and hydro-dynamical processes (w). The vertical sinking velocity of phytoplankton is taken to be a function of the ambient concentration of limiting nutrient (Slagstad 1981). Maximum sinking rates at low

nutrient concentration for diatoms and *P. pouchetii* were taken equal to 2.0 and $0.5 \, m \, d^{-1}$, respectively. The corresponding sinking rates at high nutrient concentrations were 0.1 and zero.

The model has six state variables which are described by equation (1). These are "diatoms" (Di), "*P. pouchetii*" (Ph), "nitrate" (N), "ammonium" (A), "silicic acid" (Si), and a constituent called "sinking phytoplankton" (Sp). The biological term for diatoms has the form

$$f_{biol}^{Di} = f_I^{Pi}(T, I_z, I_o) \, G^{Di}(N, A, Si) \, Di - \phi_r^{Di} Di$$
$$- q^z(Di) - f_{sed}^{Di}(N, A, Si) \, Di \qquad (2)$$

The first term on the right hand side of the equation represents growth, the second term respiration, the third term losses due to grazing by zooplankton and the last term changes in the physiological status of phytoplankton which is transformed from growing into a sinking state. $f_I^{Pi}(T, I_z)$ is the functional relationship between growth rate, temperature and light

$$f_I^{Di} = P_{Di}(T) \left(1 - \exp\{\frac{\alpha_{Di}^C I_z}{P_{Di}}\} \right) \qquad (3)$$

and

$$P_{Di}(T) = P_{Dio}^C \exp(0.0582 \, T) \qquad (4)$$

where P_{Dio}^C is the maximum carbon-specific growth rate $[h^{-1}]$ at temperature $T = 0°C$ and α_{Di}^C is the carbon-specific photosynthetic efficiency $[h^{-1}(\mu mol \, m^{-2} \, s^{-1})^{-1}]$. The upper bound on the growth rate follows an equation proposed by Eppley (1972), but parameter values are modified by data obtained from field studies (Sakshaug 1977) and field dialysis cultures (Hegseth & Sakshaug 1982) of *Skeletonema*. The photosynthetic efficiency and the Chlorophyll: Carbon ratio is a function of the photo-adaptational status of the algal cells (Slagstad 1982; Falkowski & Owens 1980; Falkowski 1980):

$$\alpha_{Di}^C = \frac{a_2 + a_1 \log I_o}{I_o}$$
$$40 < I_o < 500 \, \mu mol \, m^{-2} \, s^{-1} \qquad (5)$$

$$\frac{Chl}{C} = \frac{a_3 - a_4 \log I_o}{I_o}$$
$$40 < I_o < 500 \, \mu mol \, m^{-2} \, s^{-1} \qquad (6)$$

where I_o is the irradiance to which the phytoplankton is adapted; a_1, a_2, a_3 and a_4 are par-

ameters. The allowed range for photo-adaptation is 40–500 μmol m⁻² s⁻¹.

The rate of adaptation is assumed to be proportional to the difference between the present level of light adaptation and the irradiance or, if the irradiance is low, proportional to the irradiance (Slagstad 1982; Falkowski 1980)

$$\frac{dI_o}{dt} = \min\left\{-g_1 \frac{Chl}{C} I_z, g_o (I_z - I_o)\right\}$$

where g_1 and g_o are parameters. With the parameters used (Table 1), the range of α_{Di}^C is 0.0002 to 0.0013 [h⁻¹ (μmol m⁻² s⁻¹)⁻¹] for light- and shade-adapted cells respectively, and the corresponding Chl:C-ratios are 0.013 and 0.04. For *P. pouchetii* the range of α_{Ph}^C is 0.00017 to 0.00075 for light and shade adapted cells respectively, and the corresponding Chl:C-ratios are 0.007 and 0.02. These values are in the range found for phytoplankton from the Barents Sea (Verity et al. 1991 this volume). Reduction in growth by depletion of silicate, nitrate or ammonia is cal-

culated by

$$G^{Di}(N, A, Si) = \min\left\{\frac{Si}{k_{Si} + Si}, \frac{N}{k_N + N}\right.$$

$$\left. \times e^{-\psi A} + \frac{A}{k_A + A}\right\} \qquad (7)$$

where Si, N, and A are concentrations of silicic acid, nitrate, and ammonia, respectively. k_{Si}, k_N, and k_A are the corresponding half saturation constants. In accordance with Droop (1974), equation (7) expresses that the limiting nutrient is the one that predicts the lowest growth rate. The expression $e^{-\psi A}$ describes that uptake of nitrate is suppressed by the presence of ammonia (Walsh & Dugdale 1972). ψ is a parameter.

The transition rate of diatoms into the state called "sinking phytoplankton" is a function of the limiting nutrient:

$$f_{sed}^{Di}(N, A, Si) = d_{mn} + (d_{mx} - d_{mn})$$

$$\times \exp\left(-\frac{G^{Di}}{d_G}\right) \qquad (8)$$

Table 1. Parameters used in the 1-D model simulations.

Symbol	Value Diatoms	Value *P. pouchetii*	Unit	Meaning
P_o^C	0.68	0.48	h⁻¹	Maximum carbon specific photosynthetic rate at 0°C
k_N	0.5	0.5	mmol m⁻³	Half saturation constant of nitrate
k_A	0.5	0.5	mmol m⁻³	Half saturation constant of ammonium
k_{Si}	0.5	0.5	mmol m⁻³	Half saturation constant of silicate
ψ	1.4	1.4	(mmol m⁻³)⁻¹	Parameter concerning depression of nitrate uptake in presence of ammonium
a_1	0.034	0.02	h⁻¹	Parameters describing the relationship
a_2	0.001	0.001	h⁻¹	between α^C and level of light adaptation
a_3	0.081	0.026		Parameters describing the relationship
a_4	0.026	0.012		between the Chl:C-ratio and level of photo adaptation
g_0	0.006	0.006	h⁻¹	Rate of adaptation at medium and high irradiance
g_1	0.093	0.093	h⁻¹	Rate of adaptation per unit Chl:C-ratio at low irradiance
d_{mn}	0.0004	0.0008	h⁻¹	Parameters describing the relationship
d_{mx}	0.008	0.008	h⁻¹	between the rate of sedimentation and
d_G	0.2	0.3	—	concentration of the limiting nutrient
$\frac{N}{C}$	0.159	0.159	—	atomic N:C-ratio
$\frac{Si}{C}$	0.08	—	—	atomic Si:C-ratio
ϕ_r	0.002	0.003	h⁻¹	Rate of respiration
w_{∞}	0.0028	0	h⁻¹	Sinking rate at high nutrient concentration
w_0	0.08	0.02	h⁻¹	Sinking rate at low nutrient concentration

where d_{mn} and d_{mx} are minimum and maximum rates of transition, respectively; d_G is a parameter. The transition rate increases rapidly when the nutrients become depleted. Observations from the Barents Sea indicate that diatoms and *P. pouchetii* may, during certain conditions, sink out of the euphotic zone at a high rate depending on the physiological conditions of the algal cells. Sinking diatoms are represented mainly by resting spores, whereas *P. pouchetii* consists of colonies usually infected by bacteria (Wassmann et al. 1990). "Sinking phytoplankton" has been given relatively high velocity ($24 \, \text{m d}^{-1}$) out of the euphotic zone (Table 1).

The biological terms for the other state variables are similar to the description above. The chemical composition (except for chlorophyll content) of the phytoplankton is assumed to be constant (Table 1). Following are the biological terms for each state variable, i.e. right hand side of equation (1):

Diatoms, Di

$$f_{biol}^{Di} = f_I^{Di} \, (T, I_z, I_o) \, G^{Di} \, (N, A, Si)$$

$$\times \, Di - \phi_r^{Di} \, Di - q^z \, (Di) - f_{sed}^{Di} \, (N, A, Si) \, Di$$

Phaeocystis pouchetii, Ph

$$f_{biol}^{Ph} = f_I^{Ph} \, (T, I_z, I_o) \, G_N^{Ph} \, (N, A)$$

$$\times \, Ph - \phi_r^{Ph} \, Ph - q^z \, (Ph) - f_{sed}^{Ph} \, (N, A, Si) \, Ph$$

Nitrate, N

$$f_{biol}^{N} = - \, Di \, f_I^{Di} \frac{G^{Di}}{G_N^{Di}} \frac{N}{k_N^{Di} + N}$$

$$\times \, e^{-\psi^{Di}A} - Ph \, f_I^{Ph} \frac{N}{k_N^{Ph} + N} \, e^{-\psi^{Ph}A}$$

Ammonium, A

$$f_{biol}^{A} = E^z$$

$$- \left(Di \, f_I^{Di} \frac{G^{Di}}{G_N^{Di}} \frac{A}{k_A^{Di} + A} + Ph \, f_I^{Ph} \frac{A}{k_A^{Ph} + A} \right)$$

Silicic acid, Si

$$f_{biol}^{Si} = -Di \, f_I^{Di} \frac{Si}{N} G^{Di}$$

Sinking phytoplankton, Sp

$$f_{biol}^{Sp} = Di \, f_{sed}^{Di} + Ph \, f_{sed}^{Ph}$$

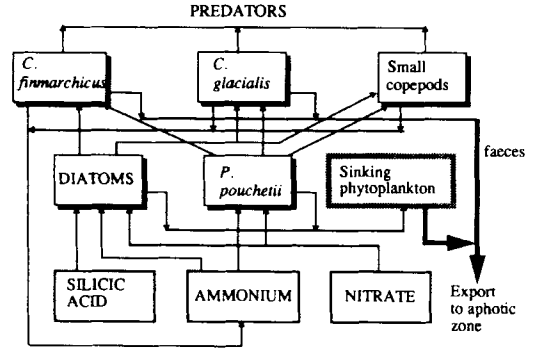where E^z is the rate of ammonium excretion from the mesozooplankton, *C. finmarchicus* and *C.*

Fig. 1. Trophic levels and biological interactions represented in the 1-D model.

glacialis; $G_N(N,A)$ is the relative reduction in growth rate due to low ammonium and nitrate concentration if no other nutrient is limiting

$$G_N \, (N, A) = \frac{N}{k_N + N} e^{-\psi A} + \frac{A}{k_A + A};$$

$\frac{Si}{N}$ is the atomic Si:N-ratio. See Table 1 for parameter values.

The box labelled "small copepods" in Fig. 1 represents mesozooplankton such as *Pseudocalanus* spp. and *Oithona* spp. We do not model dynamic growth of these species, but assume a linear increase in total biomass from 1 April ($0.05 \, \text{g C m}^{-2}$) to 1 October ($0.35 \, \text{g C m}^{-2}$; Norrbin pers. commun.). In order to simulate the relatively high turnover rate for these animals, we assume a 25% loss of biomass d^{-1} which has to be compensated for by grazing and an assimilation efficiency of 80% which has been found for the much larger copepod *C. finmarchicus* from this area (Tande & Slagstad 1985). The mesozooplankton is moreover assumed to feed only in the upper 50 m of the water column and the nitrogen fraction of all losses ends up as ammonium at the same depth it was grazed.

Photosynthetically active irradiance (PAR) at the surface is calculated from the theoretical height of the sun at a latitude of 75°N. The average reduction of insolation due to clouds is assumed to be 50% according to data obtained at Bjørnøya by the Norwegian Meteorological Institute (DNMI). Half of this is assumed to constitute PAR. Reflection loss from the surface is 5–10%, depending on the solar elevation.

The attenuation coefficient, k, of light in the water column is described by Parsons et al. (1983):

$$k = \{k_w + 0.0088\,Chl + 0.054\,(Chl)^{\frac{2}{3}}\}/\bar{\mu} \qquad (9)$$

where k_w (m^{-1}) represents the attenuation coefficient for pure seawater (Smith & Baker 1981), Chl is the concentration of chlorophyll a; $\bar{\mu}$ is the average cosine of the light field and equals 0.6 (Kirk 1983).

The initial conditions of nitrate, silicic acid and ammonia were set at 11; 5.5 and 0.1 mmol m^{-3}, respectively, which are average values for the Barents Sea in winter. Concentrations of diatoms and *P. pouchetii* were set at 0.07 and 0.05 mg Chl m^{-2}, respectively, at the start of the simulation 1 March.

The equations are solved by a finite difference method by dividing the water column into 5 m layers. Each layer is assumed to be well mixed and the exchange between them is determined by the vertical turbulent mixing coefficients. The time step is 1 hour and the simulations were performed on a MicroVax computer.

3-D Model

Due to limited computer capacity, the 3-D phytoplankton model is a simplified version of the 1-D model. The state variables are phytoplankton (P) and nitrate (N). Their distribution is described by

$$\frac{\partial\theta}{\partial t} + u\frac{\partial\theta}{\partial x} + v\frac{\partial\theta}{\partial y} + w\frac{\partial\theta}{\partial z} - \frac{\partial}{\partial z}\left(K_z\frac{\partial\theta}{\partial z}\right)$$

$$- K_H\frac{\partial^2\theta}{\partial x^2} - K_H\frac{\partial^2\theta}{\partial y^2} = f_{biol}^{3D} \qquad (10)$$

where $\theta\,(x, y, z, t)$ is the concentration of phytoplankton or nitrate and x, y and z are the two horizontal and the vertical coordinates, while u, v and w are the corresponding velocities. K_z and K_H are the horizontal and vertical turbulent mixing coefficients. The biological term, f_{biol}^{3D}, is described by

$$f_{biol}^{3D} = P_P\,(T)\left\{1 - \exp\left(\frac{-\alpha_P^C I_z}{P_P(T)}\right)\right\}$$

$$\times \frac{N}{k_N + N}P - \phi_r^{3D}P \qquad (11)$$

and

$$P_P(T) = P_{P0}^C\exp\,(0.0582T). \qquad (12)$$

The variable definition is the same as for equations (3) and (4). The relationship between irradiance and growth rate is a formulation similar to one by Platt & Jassby (1976). The parameters α^C [$= 0.0005$ h^{-1} (μmol m^{-2} s^{-1})$^{-1}$] and P_{P0}^C [$= 0.028$ h^{-1}] at 0°C, corresponding to a maximum growth rate of 0.67 d^{-1} (continuous light), are the initial slope and the maximum growth rate of the growth-irradiance relationship. The maximum growth rate is a function of the temperature according to Eppley (1972). The half saturation constant of nitrate k_N is equal to 0.5 mmol m^{-3}.

ϕ_r^{3D} is the loss rate due to respiration, grazing and sedimentation. We have chosen the value 0.1 d^{-1} for this rate, when the nitrate concentration is >0.5 mmol m^{-3}. To simulate increases in loss due to sedimentation, ϕ_r^{3D} is set equal to 0.2 d^{-1} for nitrate concentrations below 0.5 mmol m^{-3}. The Chl:C ratios is kept constant at 0.04 (w/w).

Irradiance in the water column has been calculated in the same way as for the 1-D model.

In order to solve equation (10) it is necessary to know five hydrodynamical variables (u, v, w, K_z, K_H). These variables are taken from a 3-D hydrodynamical model which calculates velocities and turbulent mixing coefficients as a dynamic function of bottom topography, density (temperature and salinity), wind and atmospheric pressure (Støle-Hansen & Slagstad 1991 this volume).

Initial concentrations of nitrate and chlorophyll were set at 11 mmol N m^{-3} and 0.1 mg Chl m^{-3}.

The 3D-model is divided into 12 layers. The upper 5 layers have a depth of 10 m; the next two layers depths of 20 and 30 m. The depth between 100 and 200 m is divided into two layers of 50 m each, and below 200 m there are three layers of 100 m each. The maximum depth is 500 m. Horizontal grid spacing is 20 km and the time step is 1 hour. Since the model domain (Fig. 2) covers an area of 1600 × 1400 km, there are 5600 grid points. The simulations were performed on a SUN SPARC 2 work station.

Results and discussion

Production dynamics in Atlantic Water

The vertical turbulent mixing coefficient is the most important physical parameter in a 1-D model. This parameter is a dynamic function of
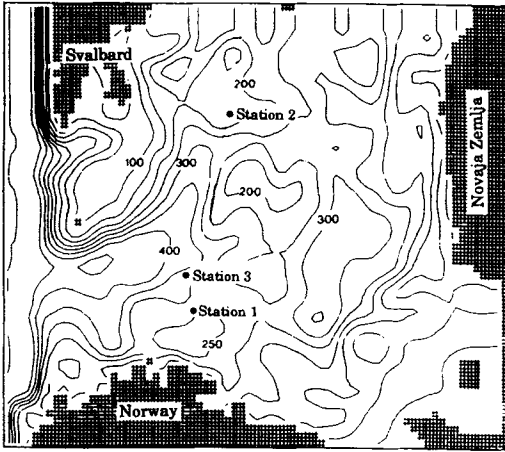
Fig. 2. Bottom topography of the model area. Isobath distance is 50 m. Station 1 and 2 indicate positions from where input data are taken for the "Atlantic" and "Arctic" simulations, respectively. Station 3 gives the position of the time series shown from the 3-D simulation run.

Fig. 4. A. Variations in K_z with depth in spring (solid line) and summer (broken line). B. Average measured (broken line) and simulated (solid line) temperature profile at 7 June 1983.

water density structure and wind speed. The density strongly depends on heat flux through the air-sea interface and on supply of fresh water from land run-off or melting ice. There are not enough data on thermodynamic energy exchange between sea surface and atmosphere available to implement one of the existing vertical turbulent mixing models (Denman & Miyake 1973; Kraus 1977). Surface temperature measurements obtained by DNMI through satellites usually exhibit a slow increase in temperature during the spring and a rapid increase in May or June (Fig. 3). We interpret this time response as follows: The surface temperature increases slowly when the wind-mixed layer is deep. After formation of a thermocline, the upper mixed water column is

Fig. 3. Surface temperatures during the spring and summer obtained through satellites at position 73°30'N 30°30'E for the years 1981–1983.
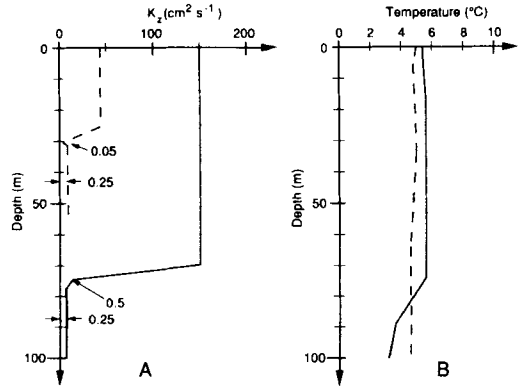
shallow and needs less energy input to increase its temperature. We therefore assume the date of thermocline formation to be the same as that when the first sign of rapid increase in sea surface temperature is observed. The input data for this station are taken from position 72°30'N 30°00'E.

Atlantic Water can be mixed down to the bottom or more than 200 m during the winter. Based on available data (Rey & Loeng 1985; Loeng 1989), an average mixed depth of 75 m is assumed during the early spring (April–May), decreasing to about 30 m after the thermocline is formed. The depth-dependent variation of K_z is calibrated by allowing the measured sea surface temperatures to mix downward in the water column and subsequent comparison with the hydrographic data (Fig. 4).

As the surface irradiance increases during the spring, there is a steady increase in primary production (Fig. 5A). The sedimentation at 75 m does increase when the biomass increases, but sinking of phytoplankton does not become pronounced until the nutrients are depleted. Grazing by *C. finmarchicus* is low in the spring when most of the population consists of nauplii and small copepodites, but increases in June as the biomass of the new generation increases (Tande & Slagstad 1992). The mixing becomes shallower in early June. This reduces the respiration losses and causes an increase in the average irradiance in the upper mixed layer. This in turn results in higher primary production until the advent of nutrient exhaustion (Fig. 5B).

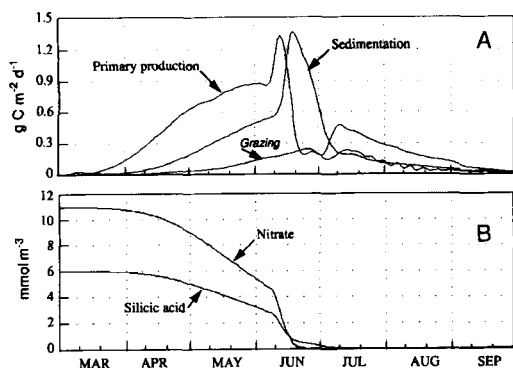According to surface temperature data, a thermocline was formed quite early in 1981 compared

Fig. 5. A. Simulated daily primary production, rate of sedimentation through a level at 75 m, and grazing by the main herbivore (*C. finmarchicus*) in Atlantic water. B. Surface concentration of nitrate and silicic acid as a function of time.

Fig. 7. Simulated concentration of chlorphyll (mg m^{-3}) as a function of depth and time in Atlantic Water. Input data from 1983.

with 1982 and 1983. This year had a cold winter and the ice border was more southerly distributed than normal (Midttun & Loeng 1987). The early formation of a thermocline in 1981 was therefore caused by the release of meltwater into areas usually characterised by Atlantic Water. The year 1983, which had a winter with less ice than normal, probably experienced a late formation of thermocline. High production lasted according to these simulations three weeks longer in 1983 than in 1981 (Fig. 6).

Fig. 6. A. Simulated primary production (g C m^{-2} d^{-1}) in a vertical water column of Atlantic Water. B. Surface concentration of chlorophyll (mg m^{-3}) using surface temperature for three different years as input.
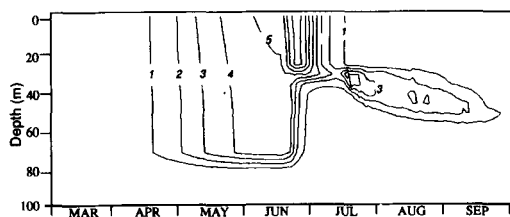
Gross integrated primary production during the spring and summer is 80–100 g C m^{-2} yr^{-1}, depending on the date for thermocline formation. New production (based on nitrate) is about 50–60 g C m^{-2} yr^{-1}. This is somewhat higher than calculated on the basis of P-I curves (Rey et al. 1987). The concentration of phytoplankton increases slowly during April and May, but more rapidly near the surface when the thermocline forms (Figs. 6 and 7). After the surface chlorophyll concentration has decreased by grazing and sedimentation, light can penetrate below the thermocline so that the primary production increases again. This results in a chlorophyll maximum near the nutricline. Simulated vertical profiles of nitrate correspond reasonably well with measurements (Fig. 8), indicating that the vertical mixing coefficients are of the right order of magnitude.

Massive reduction in the silicic acid concentration below the nitracline is common over extensive areas of the Barents Sea (Rey & Skjoldal 1987; Rey & Loeng 1985). Consumption of silicic acid below the euphotic zone by sedimenting diatom blooms has been suggested as a mechanism to explain this (Rey & Skjoldal 1987). Model simulations that do not include this mechanism may show a similar vertical distribution of nitrate and silicic acid (Fig. 9). This is due to reduced uptake of nitrate with increasing concentration of ammonium. Diatoms are able to almost deplete a 70 m deep water column for silicic acid while the nitrate level exceeds 3 mmol m^{-3}. When the thermocline is formed, the nitrate in the upper 30 m is depleted by the *P. pouchetii* within a few days and we obtain a silicacline which is considerable deeper than the nitracline (Fig. 9).

A typical feature of the vertical structure of the Barents Sea phytoplankton community is the formation of a chlorophyll maximum below the
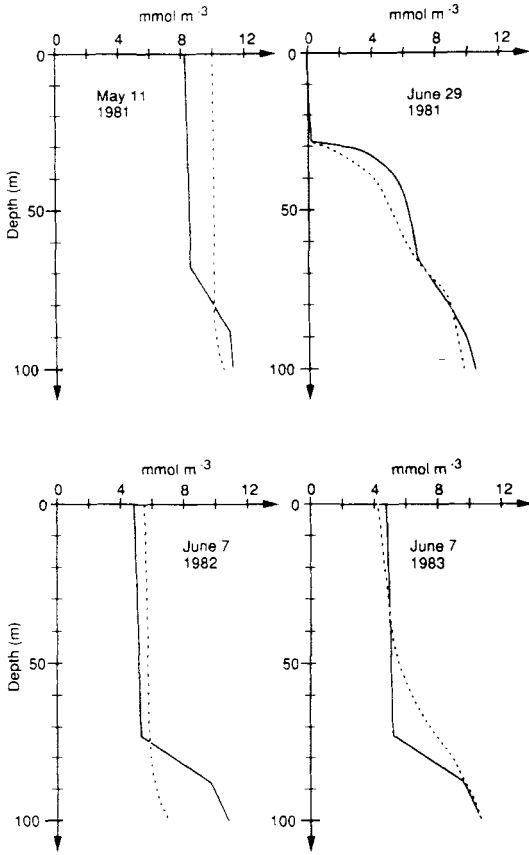
Fig. 8. Measured (broken lines) and simulated (solid lines) vertical profiles of nitrate. The data are based on averages for Atlantic waters (Skjoldal et al. 1987; Rey & Loeng 1985).

wind-mixed layer. Necessary conditions for creating a maximum are strong vertical stability and nutrient depletion in the surface waters. In the meltwater zone south of the ice border, the chlorophyll maximum may be well-established in early June (Skjoldal et al. 1987). In Atlantic Water, this takes place in June or July depending on the date of thermocline formation (Fig. 7). When estimating chlorophyll concentrations on the basis of surface chlorophyll by means of remote sensing, one should be aware of this.

Annual production of *C. finmarchicus* is 7–12 g C m^{-2}, depending on the abundance of overwintering females (Tande & Slagstad 1992).

Production dynamics in Arctic Water

Arctic Water masses are usually covered by ice during the spring. Before melting takes place, the water column is mixed to 60–70 m depth or more. Melting of ice releases freshwater and establishes a pycnocline at 10–15 m depth after the ice has gone. There is a gradient in salinity below the pynocline (Fig. 10) indicating a low value of the vertical eddy diffusion mixing coefficient.

The most pronounced effect of ice on phytoplankton growth is the strong attenuation of light caused by ice thickness and snow cover. This will of course vary during the spring and with the distance from the ice edge. Open water (leads) is more or less a constant feature of the area. Since there is a nonlinear relationship between light and
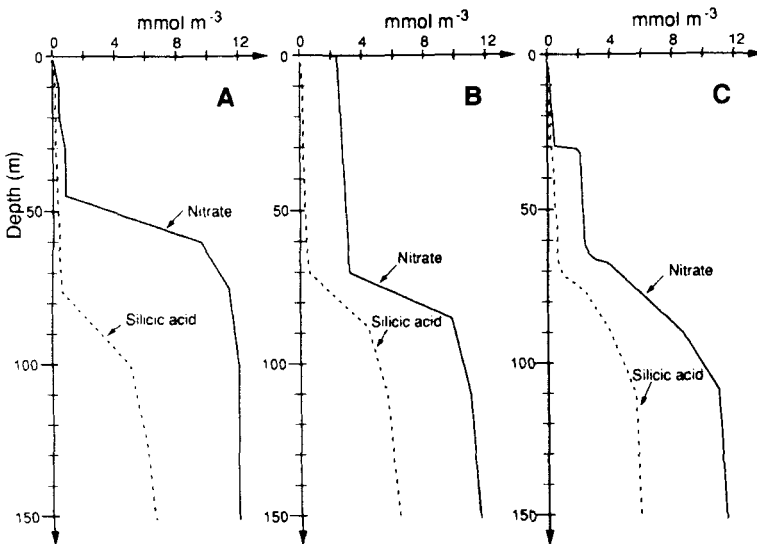

Fig. 9. A. Measured vertical structure of nitrate and silicic acid at a late phase of the spring bloom (75°20'N 36°00'E, 7 June 1984, from Rey & Skjoldal 1987). B–C. Simulated vertical structures before and after formation of a thermocline at 30 m.
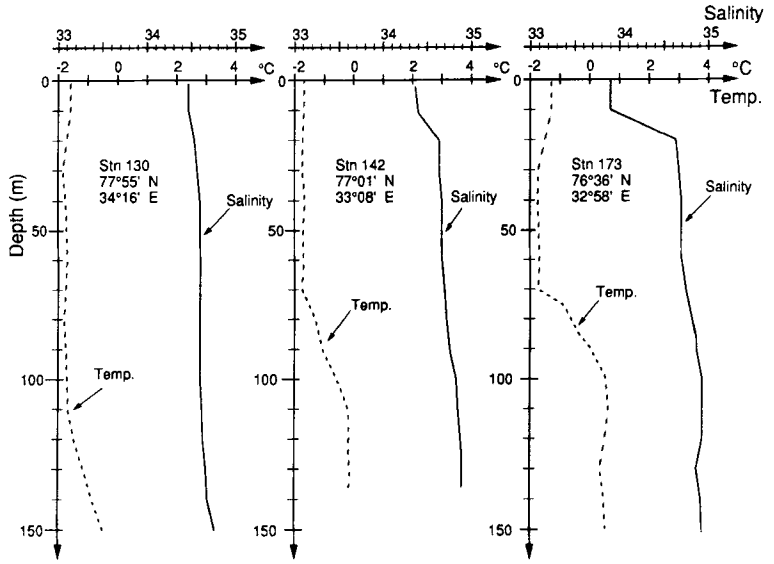
Fig. 10. Typical vertical profiles of temperature and salinity at selected stations in ice-covered areas of the Barents Sea (Lance cruise, June 1983).

algal growth, the average irradiance cannot be used to calculate primary production. If we assume that horizontal mixing is sufficiently high to smear out horizontal gradients, the following relationship between diatom growth and light at a depth z can be employed

$$f_{biol}^{Di} = \{f_l^{Di}(T, I_z, I_z)(1 - \tau_c)$$
$$+ f_l(T, I_z^{ice}, I_o)\tau_c\}G^{Di}$$
$$\times (N, A, Si) - \phi_r Di - q^z (Di)$$
$$- f_{sed}^{Di}(N, A, Si)Di \qquad (13)$$

Irradiance at depth z is

$$I_z^{ice} = I_z \cdot \tau_c \qquad (14)$$

where r_c is the relative fraction of the ice-covered area, τ_c is the average transmission coefficient of irradiance through the ice. Other variables are

the same as in equation (2). The input data (ice cover and surface temperature) have been taken from position 78°40'N 33°30'E.

Daily simulated primary production increases rapidly as the ice cover becomes less compact and until the nutrients are exhausted (Fig. 11). This takes place before the ice is completely melted. A second maximum in production is observed when the concentration of phytoplankton in the mixed layer has decreased because of grazing and sinking/sedimentation so that light can penetrate into the nutrient-rich waters below the pycnocline.

Because the mixed layer in Arctic Water is usually more shallow and vertical stability more pronounced than in the Atlantic Water, the chlorophyl maximum usually becomes much more pronounced. The maximum concentration is gradually shifted into deeper water when the nutrients are depleted (Fig. 12). Simulations indi-
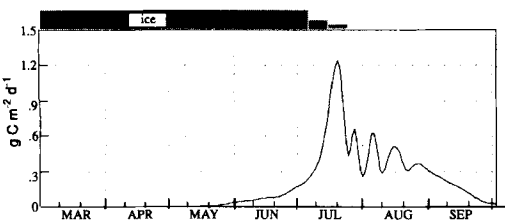

Fig. 11. Simulated primary production (g C m^{-2} d^{-1}) in a vertical water column of Arctic Water.
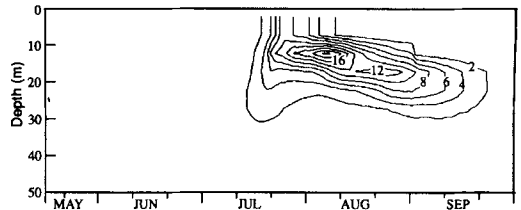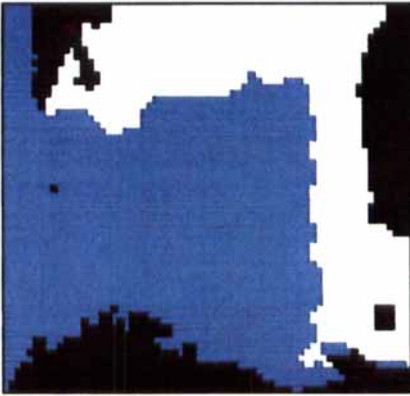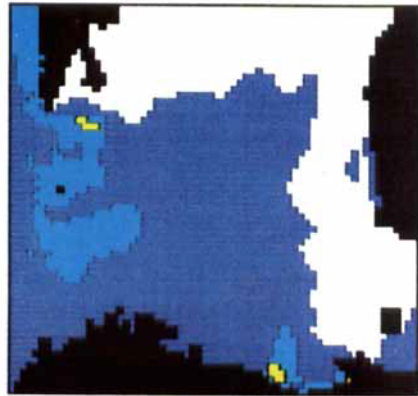

Fig. 12. Simulated concentration of chlorophyll (mg m^{-3}) as a function of depth and time in Arctic Water. Input data from 1983.
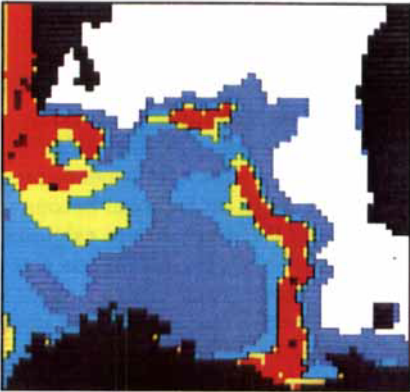
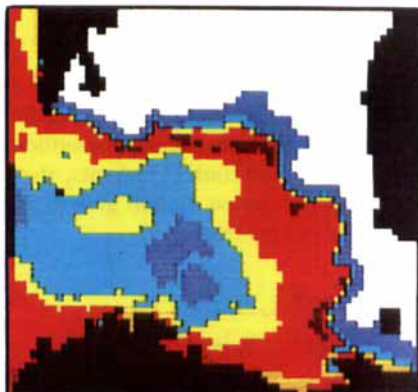0-2   2-4   4-6   6-8   8-10   10-12   12-14   14-16

Apr 5

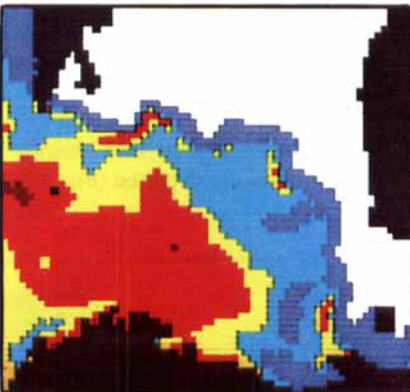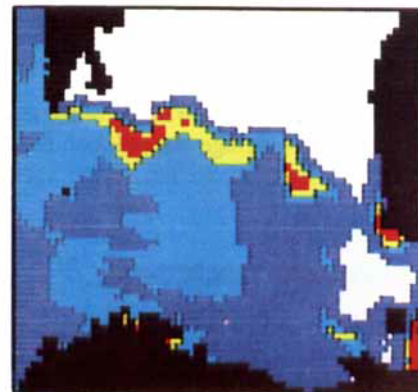Apr 19

May 3

May 17

Jun 1

Jun 14

Fig. 13. Simulated surface concentration of chlorophyll (mg m⁻³) at selected dates. The atmospheric input data (wind and radiation) were from 1983.

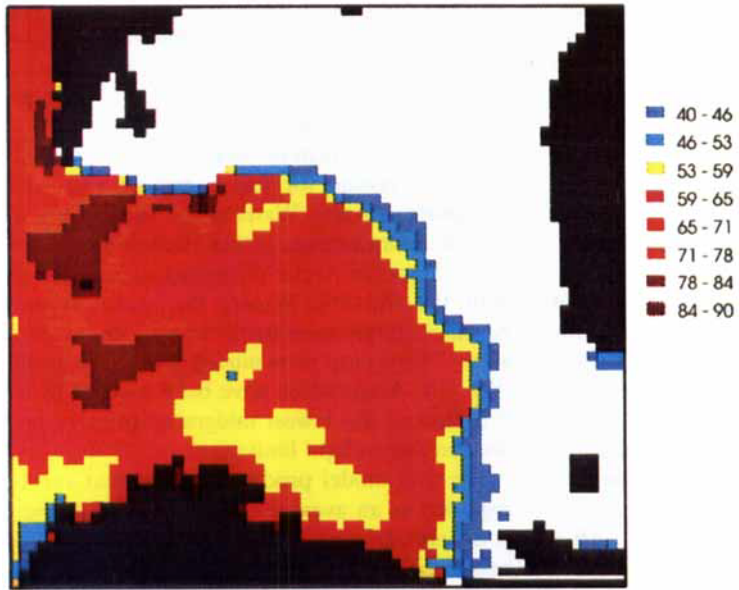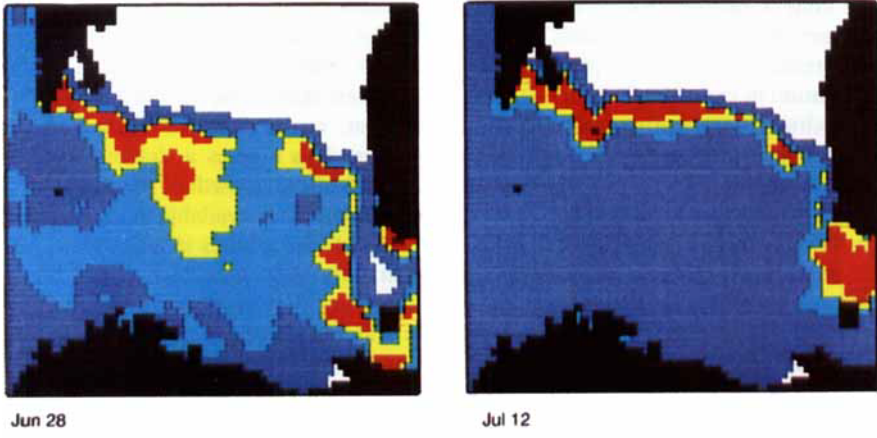Jun 28

Jul 12

■	40 - 46
■	46 - 53
■	53 - 59
■	59 - 65
■	65 - 71
■	71 - 78
■	78 - 84
■	84 - 90

Fig. 14. Integrated primary production (g C m^{-2}) from March to July.

cate a sinking velocity of the chlorophyll maximum of about 0.5 m d^{-1}. As the surface irradiance becomes lower in late summer and the chlorophyll maximum deeper, a limit is reached where the maximum cannot longer be sustained. Besides, grazing may also reduce the chlorophyll maximum. Still a maximum in chlorophyll somewhere below the pycnocline is a most pronounced feature of the summer phytoplankton community in the very stable Arctic waters.

Simulations indicate that areas which become ice-free in May may have an annual primary production of >40 g C m^{-2}, whereas areas further north that become ice-free in August probably have a production of <25 g C m^{-2}.

The main secondary producer in Arctic Water is *C. glacialis*. Simulation and sensitivity analysis indicate that the annual production is probably about the same as for *C. finmarchicus* in Atlantic waters (Slagstad & Tande 1990). However, the dynamics of these two species are quite different. When *C. finmarchicus* females die after spawning, the zooplankton biomass is reduced to a very low level before the individuals of the new generation become big enough to contribute to the biomass. When *C. glacialis* females disappear after spawning, the one-year-old animals (Stage IV) have already been growing for a while and the population biomass will not decrease.

3-D model

Temperature and salinity distributions are important initial conditions for a baroclinic, hydrodynamical model (Støle-Hansen & Slagstad 1991). These distributions are not available for the whole Barents Sea during the season when most of the phytoplankton production takes place. The best synoptic data are from the autumn. On the basis of one data set (autumn 1988), the air temperature was set far below zero (−25°C) in order to simulate winter conditions in the Barents Sea. No wind was applied. After a few months of simulations, the northern and eastern parts of the model area were covered with ice. This ice distribution is similar to that observed in early spring 1983. These simulated distributions of temperature, salinity and ice were therefore used as initial conditions for the combined hydrodynamical and biological simulations which were started 1 March.

The input data were simulated wind and atmospheric pressure fields from 1983 (performed by DNMI), air temperature, relative humidity and solar radiation at Bjørnøya. The vertical turbulent mixing coefficient was calculated as a dynamic function of wind and heat transport through the air/sea interface by using the Richardson number (Støle-Hansen & Slagstad 1991).

The wind stress moves the ice border south of the Polar Front, causing the ice to melt in the Atlantic Water. This creates a shallow layer of meltwater which allows growth of phytoplankton as soon as light becomes available in early spring (Fig. 13). The bloom reaches its maximum concentration in early May and is terminated due to nutrient limitation. The maximum concentration in Atlantic Water is, however, reached one month later, during a calm period at the end of May. A reduced growth rate due to nutrient depletion and losses soon turns the surface layer into 'blue water'.

High integrated primary production on Spitsbergenbanken (Fig. 14) is partly due to the restricted depth, which keeps the average irradiance high enough to allow early growth of phytoplankton, and partly due to the transport of nutrient-rich water from the ice-covered areas. This water has not been exposed to light and is therefore a continuous source of nutrients for areas where the current direction is off the ice edge. Southeast of Bjørnøya, there is an area which shows relatively high integrated primary production. The reason for this is mixing and small transports of Arctic Water at the surface into an eddy in Bjørnøyrenna (Støle-Hansen & Slagstad 1991). Since the Arctic Water has a lower density than the Atlantic Water, the water column becomes slightly more stable than the surrounding areas. This is most pronounced in the early spring (Fig. 13). Areas which have been covered by ice experienced the lowest integrated primary production due to light limitation.

The 1-D model produces results that can be regarded as an average for an area. Since there is no atmospheric forcing, all time series look smooth. The 3-D simulations, however, produce results that illustrate the spatial and temporal variability in primary production. Total integrated primary production is 90–120 g C m^{-2} yr^{-1} whereas new production is 70–90 g C m^{-2} yr^{-1}. This is 40–50% higher than the production estimates from the 1-D model. Time series of primary production and nitrate concentration at the surface (Fig. 15) show that wind events can increase the supply of nutrients through increased vertical
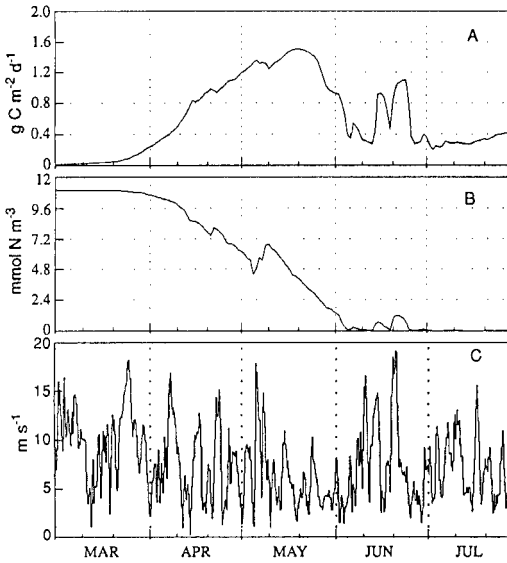
Fig. 15. Simulated daily depth integrated gross primary production (A), concentration of nitrate at the surface (B) and wind speed (C) at Station 3.

mixing. The wind event on 20 June brought nitrate into the surface layer and caused a second bloom (Fig. 13) on 28 June. These results illustrate the importance of possessing a knowledge of the history of atmospheric episodes when data from an area like the Barents Sea is being analysed.

Integrated carbon flow (Fig. 16) simulated by the 1-D model indicates that most of the primary production is exported from the euphotic zone.

Low temperatures do not seem to be a limiting factor for primary production in the Barents Sea. However, low temperatures slow down the growth of herbivores which then cannot utilise the large spring bloom stocks.

The present models seem to produce an overall picture of the phytoplankton dynamics which is in accordance with observations in the Barents Sea. The models, however, need to be verified with spatial data sets. In order to do this, more accurate input data such as thermal energy exchange between the air/sea interface, cloud cover and water density data during the spring from the whole model domain is needed.

During the spring, when grazing is low, the primary production is mainly a function of surface light and depth of mixing. Knowledge of this physical environment allows this production to easily be simulated within acceptable limits. In order to make a more reliable assessment of the dynamics of phytoplankton production, the hydrodynamical model and its input data should be improved. However, when questions are raised about species composition, for example the relation between *P. pouchetii* and diatoms, the model has very low predictive value; improvements here would call for more biological knowledge of each species and their trophic interactions.
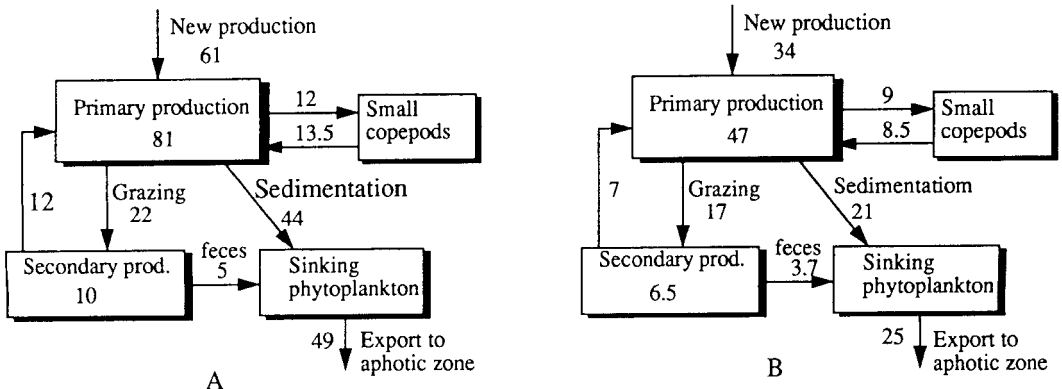
Fig. 16. Integrated carbon flow between different model compartments for average Atlantic (A) and Arctic (B) waters. The apparent carbon flow from copepods to phytoplankton is the potential primary production due to nitrogen excretion from the copepods.

References

Balchen, J. G. B. 1980: Modeling and identification of marine ecological systems with applications in management of fish resources and planning of fisheries operations. *Modeling, Identification, Control 1*. 67–68.

Båmstedt, U., Eilertsen, H. C., Tande, K., Slagstad, D. & Skjoldal, H. R. 1991: Copepod grazing and its potential impact on the phytoplankton development in the Barents Sea. Pp. 339–353 in Sakshaug, E., Hopkins, C. C. E. & Øritsland, N. A. (eds.): Proceedings of the Pro Mare Symposium on Polar Marine Ecology, Trondheim, 12–16 May 1990. *Polar Research 10(2)*.

Denman, K. L. & Miyake, M. 1973: Upper layer modifications at ocean station Papa: Observations and simulation. *J. Phys. Oceanogr. 3*, 185–196.

Droop, M. R. 1974: The nutrient status of algal cells in continuous culture. *J. Mar. Biol. Ass. U.K. 54*, 825–855.

Eppley, R. 1972: Temperature and phytoplankton growth in the sea. *Fish. Bull. 4*, 1063–1085.

Falkowski, P. G. & Owens, T. G. 1980: Light-shade adaptation. Two strategies in marine phytoplankton. *Plant. Physiol. 66*, 592–595.

Falkowski, P. G. 1980: Light-shade adaptation in the sea. Pp. 99–119 in Falkowski, P. G. (ed): *Primary productivity in the sea*. Plenum Publishing Corporation, New York.

Hegseth, E. N. & Sakshaug, E. (1982): Seasonal variation in light- and temperature-dependent growth of marine planktonic diatoms in in situ dialysis cultures in the Trondheimsfjord, Norway (63°). *J. Exp. Mar. Biol. Ecol. 67*, 199–220.

Kirk, J. T. O. 1983: *Light and photosynthesis in aquatic ecosystems*. Cambridge University Press, Melbourne. 401 pp.

Kraus, J. (ed.) 1977: *Modelling and prediction of the upper layer of the ocean*. Pergamon Press. 325 pp.

Loeng, H. 1989: Ecological features of the Barents Sea. Pp. 327–365 in Rey, L. & Alexander, V. (eds.): *Proc. 6th Conf. Com. Arct. Internat.* E. J. Brill, Leiden.

Midttun, L. & Loeng, H. 1987: Climatic variations in the Barents Sea. Pp. 13–27 in Loeng, H. (ed.): *The effect of oceanographic conditions on distribution and population dynamics of commercial fish stocks in the Barents Sea*. Proc. 3rd Soviet-Norwegian Symp., Murmansk, 26–28 May 1986.

Parsons, T. R., Takahashi, M. & Hargrave, B. 1983: *Biological oceanographic processes*. Pergamon Press, Oxford. 332 pp.

Platt, T. & Jassby, A. D. 1976: The relationship between phytosynthesis and light for natural assemblages of coastal marine phytoplankton. *J. Phycol. 12*, 421–430.

Rey, F. & Skjoldal, H. R. 1987: Consumption of silicic acid below the euphotic zone by sedimenting diatom blooms in the Barents Sea. *Mar. Ecol. Prog. Ser. 36*, 307–312.

Rey, F., Skjoldal, H. R. & Slagstad, D. 1987: Primary production in relation to climatic changes in the Barents Sea. Pp. 29–46 in Loeng, H. (ed.): *The effect of oceanographic conditions on distribution and population dynamics of commercial fish stocks in the Barents Sea*. Proc. 3rd Soviet-Norwegian Symp., Murmansk, 26–28 May 1986.

Rey, F. & Loeng, H. 1985: The influence of ice and hydrographical conditions on the development of phytoplankton in the Barents Sea. Pp. 49–64 in Gray, J. S. & Christiansen, M. E. (eds.): *Marine Biology of Polar Regions and Effects of Stress on Marine Organisms*. J. Wiley & Sons Ltd.

Sakshaug, E. (1977): Limiting nutrients and maximum growth rates for diatoms in Narragansett Bay. *J. Exp. Mar. Biol. Ecol. 28*, 109–123.

Sakshaug, E. & Slagstad, D. 1991: Light and productivity of phytoplankton in polar marine ecosystems: a physiological view. Pp. 69–85 in Sakshaug, E., Hopkins, C. C. E. & Øritsland, N. A. (eds.): Proceedings of the Pro Mare Symposium on Polar Marine Ecology, Trondheim, 12–16 May 1990. *Polar Research 10(1)*.

Skjoldal, H. R., Hassel, A., Rey, F. & Loeng, H. 1987: Spring phytoplankton development and zooplankton reproduction in the Central Barents Sea in the period 1979–1984. Pp. 59–90 in H. Loeng (ed.): *The effect of oceanographic conditions on distribution and population dynamics of commercial fish stocks in the Barents Sea*. Proc. 3rd Soviet-Norwegian Symp., Murmansk, 26–28 May 1986.

Slagstad, D. & Tande, K. S. 1990: Growth and production dynamics of *Calanus glacialis* in an Arctic pelagic food Web. *Mar. Ecol. Prog. Ser. 63*, 189–199.

Slagstad, D. 1981: Modeling and simulation of physiology and population dynamics of copepods. Effects of physical and biological parameters. *Modeling, Identification, Control 2*, 119–162.

Slagstad, D. 1982: A model of phytoplankton growth-effect of vertical mixing and adaptation to light. *Modeling, Identification, Control 3*, 111–130.

Smith, V. & Baker, K. S., 1981: Optical properties of the clearest natural waters (200–800 nm). *Appl. Optics 20*, 177–184.

Støle-Hansen, K. & Slagstad, D. 1991: Simulation of currents, ice-melting, and vertical mixing in the Barents Sea using a 3-D baroclinic model. Pp. 33–44 in Sakshaug, E., Hopkins, C. C. E. & Øritsland, N. A. (eds.): Proceedings of the Pro Mare Symposium on Polar Marine Ecology, Trondheim, 12–16 May 1990. *Polar Research 10(1)*.

Sverdrup, H. U. 1953: On conditions for the vernal blooming of phytoplankton. *J. Cons. Perm. Int. Explor. Mer 18*, 287–295.

Tande, K. & Slagstad, D. 1985: Assimilation efficiency in herbivorous aquatic organisms – the potential of the ratio method using ¹⁴C and biogenic silica as markers. *Limnol. Ocenogr. 30*, 1093–1099.

Tande, K. & Slagstad, D. 1992: Regional and interannual variations in biomass and productivity of *Calanus finmarchicus* in subarctic environments. *Oceanologia Acta*. In press.

Tande, K., Hassel, A. & Slagstad, D. 1985: Gonad maturation and possible life cycle strategies in *Calanus finmarchicus* and *Calanus glacialis* in the northern Barents Sea. Pp. 141–155 in Gray & Christiansen (eds.): *Marine Biology of Polar Regions and Effects of Stress on Marine Organisms*. J. Wiley and Sons, Ltd.

Verity, P. G., Smayda, T. J. & Sakshaug, E. 1991. Photosynthesis, excretion, and growth rates of *Phaeocystis* colonies and solitary cells. Pp. 117–128 in Sakshaug, E., Hopkins, C. C. E. & Øritsland, N. A. (eds.): Proceedings of the Pro Mare Symposium on Polar Marine Ecology, Trondheim, 12–16 May 1990. *Polar Research 10(1)*.

Walsh, J. J. & Dugdale, R. C. 1972: Nutrient submodels and simulation models of phytoplankton production in the sea. Pp. 171–191 in Kramer, J. & Allen, H. (eds.): *Nutrients in Natural Waters*. J. Wiley and Sons, New York.

Wassmann, P., Vernet, M., Mitchell, B. G. & Rey, F. 1990: Mass sedimentation of *Phaeocystis pouchetii* in the Barents Sea. *Mar. Ecol. Prog. Ser. 66*, 183–195.